Gyroscopically Induced Vibrations of Circular Plates

A. L. Schlack Jr.* and P. G. Kessel†
University of Wisconsin, Madison, Wis.

An analytical study is presented for the vibrational response of simply supported and clamped circular plates subjected to gyroscopically induced inertia loads. The plates are considered to be spinning at a constant rate while simultaneously undergoing a constant precession at a fixed angle of nutation. The equations of motion are formulated for members mounted either parallel or perpendicular to the spin axis and it is found that these equations contain distributed harmonic inertia forces whose amplitudes and frequencies are dependent on spin and precession. The solutions of these equations, obtained by Fourier-Bessel series expansions, show that the natural frequencies are reduced by the effects of spin and precession and that this effect may become appreciable for appropriate combinations of material properties and geometry. It is also shown that only certain modes of vibration respond to the gyroscopically induced inertia loading and that for members mounted parallel to the spin axis the motion is governed by a set of Mathieu equations along with the associated stability characteristics.

Nomenclature

a	=	plate radius at outer edge
$\mathbf{a}$	=	acceleration of plate element
$A_{mn},B_{mn},$ C_{mn},D_{mn}	=	amplitude coefficients
B,λ_{mn}	=	Mathieu equation coefficients
D	=	flexural rigidity of plate
E	=	modulus of elasticity
$F_{mn}(t)$	=	solution of Mathieu equation
h	=	plate thickness
I_n	=	modified Bessel functions of order n
J_n	=	Bessel functions of order n
$G(r,\beta,t)$	=	surface loading parameter for plate element
k	=	effective Winkler elastic foundation parameter
Q_{mn}	=	orthogonality constant
(r,β)	=	plate element location in polar coordinates
t	=	time
T	=	plate tension
u,v,w	=	normal plate deflections in x,y,z directions, respectively
x_1,x_2,x_3	=	general reference coordinates for plate boundaries
x,y,z	=	body reference coordinates
X,Y,Z	=	inertial reference coordinates
X_3	=	normal surface load parameter
α_{mn},γ_{mn}	=	eigenvalues associated with Bessel and modified Bessel functions, respectively
δ	=	equal to 0 for clamped plates and 1 for simply supported plates
δ_{mn},ϵ	=	nondimensional Mathieu equation coefficients
ψ,θ,ϕ	=	Euler angles
$\dot{\psi},\dot{\theta},\dot{\phi}$	=	precession, nutation, and spin, respectively
ν	=	Poisson's ratio
$\boldsymbol{\rho}$	=	position vector relative to body axes
ρ	=	mass density
τ	=	nondimensional time parameter
Ω_{mn}	=	circular frequency parameter
$\boldsymbol{\omega}$	=	angular velocity vector
$(\dot{\ })$	=	time derivative
$(\bar{\ })$	=	refers to plates mounted parallel to spin axis

I. Introduction

EULER angles are frequently used to describe the spatial orientation of the reference coordinate axes when studying general rotational motion. Thus, if an elastic structural member is mounted on an Eulerian frame of reference, it is subjected to the combined rotational effects of spin, precession, and nutation. In problems for which the spin axis is simultaneously precessing, the elastic member is subjected to gyroscopically induced distributed cyclic inertia loads. Hirshberg and Mendleson[1] and Meirovitch[2] showed this effect associated with the flexural vibrations of a thin disk clamped at its center to a spinning, precessing shaft. Johnson[3] presented an approximate solution for the case of steady precession of a spinning membrane for a nutation angle of 90° for which the gyroscopically induced inertia load appears as a constant rather than a cyclic effect. Schlack and Kessel[4] presented an analysis of the vibrational response of simply supported rectangular plates and membranes to gyroscopically induced inertia loads for constant spin, precession, and angle of nutation. The purpose of this paper is to extend the analysis of Ref. 4 to simply supported and clamped circular plates.

II. Analysis

A. Plate Equations

Consider a thin, isotropic, homogeneous, circular plate of radius a and constant thickness h as shown in Fig. 1 subjected to a uniform tension T and supported by a Winkler elastic foundation. The governing partial differential equation of motion for the plate according to elementary thin plate theory[5] is given by

$$D\nabla^2\nabla^2 w - T\nabla^2 w + kw = X_3(r,\beta,t) \qquad (1)$$

where $X_3(r,\beta,t)$ is the intensity of the normal surface load including inertia forces.

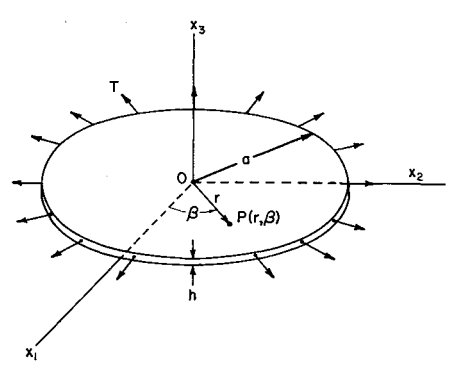

Fig. 1 Plate geometry.

Received August 22, 1968; revision received February 24, 1969.

* Professor, Department of Engineering Mechanics. Member AIAA.
† Associate Professor, Department of Engineering Mechanics.

In the absence of external normal surface loads, $X_3(r,\beta,t)$ is proportional to the component of acceleration perpendicular to the undeformed surface of the plate and is given by

$$X_3(r,\beta,t) = -\rho h a_3(r,\beta,t) \tag{2}$$

These normal inertia loads are dependent on the orientation of the plate relative to the spin axis for plates subjected to the combined effects of spin and precession. Since the more common engineering applications involve plates mounted either perpendicular or parallel to the spin axis, only these cases will be analyzed herein. However, the methods presented are equally applicable for any plate orientation.

B. Plate Mounted Perpendicular to Spin Axis

For a plate mounted perpendicular to the spin axis, the plate axes x_1, x_2, x_3 shown in Fig. 1 are oriented along the body axes x, y, z in Fig. 2, respectively. For this case, the plate deflection $w(r,\beta,t)$ is parallel to the spin axis and the transverse component of acceleration for a plate element at P is given by[4]

$$a_z(r,\beta,t) = \partial^2 w/\partial t^2 - (\dot{\psi}^2 \sin^2\theta)w + [a_{0z} + \{2\dot{\phi}\dot{\psi}\sin\theta + \dot{\psi}^2 \sin\theta\cos\theta\} r \sin(\beta + \dot{\phi}t)] \tag{3}$$

Thus, Eq. (1) may be written in the form

$$\nabla^2\nabla^2 w - \frac{T}{D}\nabla^2 w + \frac{\rho h}{D}\frac{\partial^2 w}{\partial t^2} + \frac{K}{D} w = G(r,\beta,t) \tag{4}$$

where

$$K = k - \rho h \dot{\psi}^2 \sin^2\theta \tag{5}$$

$$G(r,\beta,t) = -\frac{\rho h}{D}[a_{0z} + \{2\dot{\phi}\dot{\psi}\sin\theta + \dot{\psi}^2\sin\theta\cos\theta\} r \sin(\beta + \dot{\phi}t)] \tag{6}$$

Homogeneous solution

The homogeneous solution of Eq. (4) for nonperforated circular plates according to the method of separation of variables[6,7] may be readily shown to be of the form

$$w = \sum_{m=0}^{\infty}\sum_{n=0}^{\infty}\left[\{A_{mn}\sin n\beta + B_{mn}\cos n\beta\} J_n\left(\alpha_{mn}\frac{r}{a}\right) + \{C_{mn}\sin n\beta + D_{mn}\cos n\beta\} I_n\left(\gamma_{mn}\frac{r}{a}\right)\right] e^{i\Omega_{mn}t} \tag{7}$$

where A_{mn}, B_{mn}, C_{mn}, and D_{mn} are constants, J_n and I_n are Bessel and modified Bessel functions of order n of the first kind, respectively, and γ_{mn} and α_{mn} are related by the equation

$$\gamma_{mn}^2 - \alpha_{mn}^2 = Ta^2/D \tag{8}$$

In addition, the natural circular frequencies of the plate are given by

$$\Omega_{mn}^2 = \frac{D}{\rho h}\left(\frac{\alpha_{mn}}{a}\right)^4 + \frac{T}{\rho h}\left(\frac{\alpha_{mn}}{a}\right)^2 + \frac{k}{\rho h} - \dot{\psi}^2\sin^2\theta \tag{9}$$

Boundary conditions

The boundary conditions for simply supported plates are

$$w = 0 \text{ at } r = a \tag{10}$$

and

$$\left[\frac{\partial^2 w}{\partial r^2} + \nu\left(\frac{1}{r}\frac{\partial w}{\partial r} + \frac{1}{r^2}\frac{\partial^2 w}{\partial \beta^2}\right)\right] = 0 \text{ at } r = a \tag{11}$$

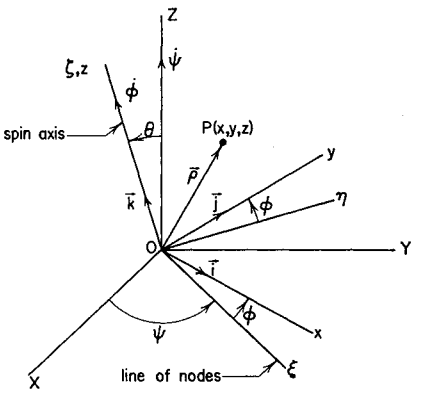

Fig. 2 Reference coordinate systems related to Euler angles.

Equation (10) is satisfied for

$$\frac{A_{mn}}{C_{mn}} = \frac{B_{mn}}{D_{mn}} = -\frac{I_n(\gamma_{mn})}{J_n(\alpha_{mn})} \tag{12}$$

In addition Eq. (11) requires that for nontrivial solutions for A_{mn}, B_{mn}, C_{mn}, and D_{mn}, the roots α_{mn} and γ_{mn} satisfy the equation

$$\alpha_{mn}\frac{J_{n+1}(\alpha_{mn})}{J_n(\alpha_{mn})} + \gamma_{mn}\frac{I_{n+1}(\gamma_{mn})}{I_n(\gamma_{mn})} = \frac{\alpha_{mn}^2 + \gamma_{mn}^2}{1-\nu} \tag{13}$$

Thus, the simultaneous solution of Eqs. (8) and (13) yields the roots α_{mn} and γ_{mn} for simply supported circular plates.

Similarly, for clamped plates the boundary conditions require that

$$w = 0 \text{ at } r = a \tag{14}$$

and

$$\partial w/\partial r = 0 \text{ at } r = a \tag{15}$$

Once again, Eq. (14) requires that

$$A_{mn}/C_{mn} = B_{mn}/D_{mn} = -I_n(\gamma_{mn})/J_n(\alpha_{mn}) \tag{16}$$

The condition of zero slope at the outer boundary according to Eq. (15) requires that

$$\alpha_{mn}\frac{J_{n+1}(\alpha_{mn})}{J_n(\alpha_{mn})} + \gamma_{mn}\frac{I_{n+1}(\gamma_{mn})}{I_n(\gamma_{mn})} = 0 \tag{17}$$

The simultaneous solution of Eqs. (8) and (17) yields the roots α_{mn} and γ_{mn} for clamped circular plates.

The solution for the roots α_{mn} and γ_{mn} for $m,n = 0,1,2$ have been presented by Wah[6] for $\nu = 0.3$ for a representative range of nondimensional tensions $\phi = T/T^*$, where $T^* = 4.2D/a^2$ for simply supported plates and $T^* = 14.68D/a^2$ for clamped plates. Accordingly, $\phi = -1$ corresponds to the radial compressive buckling load for each case.

As a result of these sets of boundary conditions, Eq. (7) may be summarized for both simply supported and clamped plates in the form

$$w = \sum_{m=0}^{\infty}\sum_{n=0}^{\infty}\left[(A_{mn}\sin n\beta + B_{mn}\cos n\beta)\left\{J_n\left(\alpha_{mn}\frac{r}{a}\right) - \frac{J_n(\alpha_{mn})}{I_n(\gamma_{mn})} I_n\left(\gamma_{mn}\frac{r}{a}\right)\right\}\right] e^{i\Omega_{mn}t} \tag{18}$$

The roots α_{mn} and γ_{mn} are given by

$$\gamma_{mn}^2 - \alpha_{mn}^2 = Ta^2/D$$

$$\alpha_{mn}\frac{J_{n+1}(\alpha_{mn})}{J_n(\alpha_{mn})} + \gamma_{mn}\frac{I_{n+1}(\gamma_{mn})}{I_n(\gamma_{mn})} = \left[\frac{\alpha_{mn}^2 + \gamma_{mn}^2}{1-\nu}\right]\delta \tag{19}$$

where $\delta = 0$ for clamped edges, $\delta = 1$ for simply supported edges, and the circular frequencies for the plate are given by Eq. (9), namely,

$$\Omega_{mn}^2 = \frac{D}{\rho h}\left(\frac{\alpha_{mn}}{a}\right)^4 + \frac{T}{\rho h}\left(\frac{\alpha_{mn}}{a}\right)^2 + \frac{k}{\rho h} - \dot{\psi}^2 \sin^2\theta$$

Nonhomogeneous solution

Using the eigenfunctions for the homogeneous solution, a series solution for the forced motion may be assumed in the following form:

$$w = \sum_{m=0}^{\infty}\sum_{n=0}^{\infty}\left[[A_{mn}(t)\sin n\beta + B_{mn}(t)\cos n\beta] \times \left\{ J_n\left(\alpha_{mn}\frac{r}{a}\right) - \frac{J_n(\alpha_{mn})}{I_n(\gamma_{mn})} I_n\left(\gamma_{mn}\frac{r}{a}\right)\right\}\right] \quad (20)$$

In addition, the roots α_{mn} and γ_{mn} are given by Eqs. (19) for either simply supported or clamped edges, insuring that the geometrical boundary conditions are satisfied.

Substituting Eq. (20) into Eq. (4) and interchanging the order of differentiation and summation gives

$$\sum_{m=0}^{\infty}\sum_{n=0}^{\infty}\left[\{(\ddot{A}_{mn} + \Omega_{mn}^2 A_{mn})\sin n\beta + (\ddot{B}_{mn} + \Omega_{mn}^2 \times B_{mn})\cos n\beta\} \left\{ J_n\left(\alpha_{mn}\frac{r}{a}\right) - \frac{J_n(\alpha_{mn})}{I_n(\gamma_{mn})} I_n\left(\gamma_{mn}\frac{r}{a}\right)\right\}\right] = \frac{D}{\rho h} G(r,\beta,t) \quad (21)$$

where the circular frequencies of the plate are given by Eq. (9).

Multiplying both sides of Eq. (21) by

$$\left\{ J_p\left(\alpha_{ps}\frac{r}{a}\right) - \frac{J_p(\alpha_{ps})}{I_p(\gamma_{ps})} I_p\left(\gamma_{ps}\frac{r}{a}\right)\right\}\sin p\beta$$

and integrating over the surface of the plate, by virtue of the orthogonality properties discussed in the Appendix, one obtains

$$\ddot{A}_{mn} + \Omega_{mn}^2 A_{mn} = \frac{D}{\rho h Q_{mn}}\int_0^{2\pi}\int_0^a G(r,\beta,t)\left\{ J_n\left(\alpha_{mn}\frac{r}{a}\right) - \frac{J_n(\alpha_{mn})}{I_n(\gamma_{mn})} I_n\left(\gamma_{mn}\frac{r}{a}\right)\right\}(\sin n\beta) r dr d\beta \quad (22)$$

Similarly,

$$\ddot{B}_{mn} + \Omega_{mn}^2 B_{mn} = \frac{D}{\rho h Q_{mn}}\int_0^{2\pi}\int_0^a G(r,\beta,t)\left\{ J_n\left(\alpha_{mn}\frac{r}{a}\right) - \frac{J_n(\alpha_{mn})}{I_n(\gamma_{mn})} I_n\left(\gamma_{mn}\frac{r}{a}\right)\right\}(\cos n\beta) r dr d\beta \quad (23)$$

where

$$Q_{mn} = \pi\int_0^a \left\{ J_n\left(\alpha_{mn}\frac{r}{a}\right) - \frac{J_n(\alpha_{mn})}{I_n(\gamma_{mn})} I_n\left(\gamma_{mn}\frac{r}{a}\right)\right\}^2 r dr \quad (24)$$

Therefore, for clamped edges,

$$(Q_{mn})_c = \pi a^2[J_n^2(\alpha_{mn}) - (Ta^2/D\pi_{mn}^2)\{\tfrac{1}{2}J_{n+1}^2(\alpha_{mn}) + J_{n+1}(\alpha_{mn})J_n'(\alpha_{mn})\}] \quad (25)$$

and for simply supported edges

$$(Q_{mn})_s = (Q_{mn})_c - \frac{\pi a^2}{1-\nu}\left[\left\{2 + \frac{(\alpha_{mn}^2 + \gamma_{mn}^2)^2}{2\gamma_{mn}^2}\right\} J_n^2(\alpha_{mn}) + \alpha_{mn}\frac{\alpha_{mn}^2 + \gamma_{mn}^2}{\gamma_{mn}^2} J_n(\alpha_{mn})J_n'(\alpha_{mn})\right] \quad (26)$$

where α_{mn} and γ_{mn} are obtained from Eq. (19) for $\delta = 0$ and 1, respectively.

Integrating the right-hand sides of Eqs. (22) and (23), we obtain

$$\begin{aligned} \ddot{A}_{mn} + \Omega_{mn}^2 A_{mn} &= A(m,n,t) \\ \ddot{B}_{mn} + \Omega_{mn}^2 B_{mn} &= B(m,n,t) \end{aligned} \quad (27)$$

where

$$A(m,n,t) = \begin{cases} 0; \text{ for } n \neq 1 \\ -\dfrac{\pi a^3}{Q_{m1}}\{2\dot{\phi}\dot{\psi}\sin\theta + \dot{\psi}^2\sin\theta\cos\theta\} \times \left\{\dfrac{J_2(\alpha_{m1})}{\alpha_{m1}} - \dfrac{J_1(\alpha_{m1})}{I_1(\gamma_{m1})}\dfrac{I_2(\gamma_{m1})}{\gamma_{m1}}\right\}\cos\dot{\phi}t \\ \qquad \text{for } n = 1 \end{cases} \quad (28)$$

$$B(m,n,t) = \begin{cases} 0; \text{ for } n \neq 0, 1 \\ -\dfrac{\pi a^3}{Q_{m1}}\{2\dot{\phi}\dot{\psi}\sin\theta + \dot{\psi}^2\sin\theta\cos\theta\} \times \dfrac{J_2(\alpha_{m1})}{\alpha_{m1}} - \dfrac{J_1(\alpha_{m1})}{I_1(\gamma_{m1})}\dfrac{I_2(\gamma_{m1})}{\gamma_{m1}}\sin\dot{\phi}t \\ \qquad \text{for } n = 1 \\ -\dfrac{2\pi a^2}{Q_{m0}}\left\{\dfrac{J_1(\alpha_{m0})}{\alpha_{m0}} - \dfrac{J_0(\alpha_{m0})}{I_0(\gamma_{m0})}\dfrac{I_1(\gamma_{m0})}{\gamma_{m0}}\right\} a_{0z}; \text{ for } n = 0 \end{cases} \quad (29)$$

Thus, it is apparent that only the modes corresponding to $n = 1$ are excited by the gyroscopically induced harmonic inertia loads. Moreover, Eqs. (27) may be added in quadrature to show that for $n = 1$, the modal profile rotates at the spin velocity $\dot{\phi}$ relative to the body axes. The normal acceleration a_{oz} of the center of the plate excites the axisymmetric modes of vibration corresponding to $n = 0$ as shown by Eq. (29). For all other cases, the plate undergoes free vibration.

The particular solutions of Eqs. (27) for $a_{oz} = 0$ are given by

$$\begin{aligned} A_{mn} &= A(m,n,t)/(\Omega_{mn}^2 - \dot{\phi}^2) \\ B_{mn} &= B(m,n,t)/(\Omega_{mn}^2 - \dot{\phi}^2) \end{aligned} \quad (30)$$

Thus, Eq. (30), along with the well-known homogeneous solutions of Eqs. (27), together with Eq. (20) completes the solution for a circular plate mounted perpendicular to the spin axis.

It is interesting to note from Eq. (9) that for any mode of vibration, the natural frequency of the plate is reduced by the effect of the precession $\dot{\psi}$ for the angle of nutation θ different from 0 or π. For $T = k = 0$, the reduction in natural frequency is dependent on the ratio of $\dot{\psi}\sin\theta$ to the flexural rigidity parameter $(D/\rho h)^{1/2}(\alpha_{mn}/a)^2$. As a numerical example, consider a simply supported aluminum plate for which $m = n = 0$, $a = 20$ in., and $h = \frac{1}{16}$ in., which results in $(D/\rho h)^{1/2}(\alpha_{mn}/a)^2 = 46$. Thus, this example illustrates that the reduction in natural frequency can become appreciable for appropriate combinations of material properties and geometry.

By taking $D = k = 0$ in Eq. (9), one obtains the natural frequency for a precessing membrane given by

$$\Omega_{mn}^2 = (T/\rho h)(\alpha_{mn}/a)^2 - \dot{\psi}^2\sin^2\theta \quad (31)$$

for which it becomes apparent that the precentage reduction in natural frequency may become very large, especially for low values of initial tension. Thus, Eqs. (9) and (31) give the design criteria for satisfying natural frequency design specifications, taking precession and nutation into account.

C. Plate Mounted Parallel to Spin Axis

For a plate mounted parallel to the spin axis, the plate axes x_1,x_2,x_3 shown in Fig. 1 are oriented along the z,x,y axes in Fig. 2, respectively. Thus, the undeformed plane of the plate (Fig. 2) is the xz plane and the plate deflection, referred to in this case as $v(r,\beta,t)$ is in the y direction. The transverse component of acceleration of the plate element $P(r,\beta)$ is given by[4]

$$a_y(r,\beta,t) = \partial^2 v/\partial t^2 - v\{(\dot\phi + \dot\psi\cos\theta)^2 + \dot\psi^2\sin^2\theta\sin^2\dot\phi t\} + [a_{oy} + (\dot\psi^2\sin\theta\cos\theta)r\cos\beta\cos\dot\phi t + (\tfrac{1}{2}\dot\psi^2\sin^2\theta)r\sin\beta\sin 2\dot\phi t] \quad (32)$$

As a result, the governing partial differential equation of motion given by Eq. (1) becomes

$$\nabla^2\nabla^2 v - \frac{T}{D}\nabla^2 v + \frac{\rho h}{D}\frac{\partial^2 v}{\partial t^2} + \frac{\bar K(t)}{D}v = \bar G(r,\beta,t) \quad (33)$$

where

$$\bar K(t) = k - \rho h\left\{(\dot\phi + \dot\psi\cos\theta)^2 + \frac{\dot\psi^2\sin^2\theta}{2}(1 - \cos 2\dot\phi t)\right\} \quad (34)$$

$$\bar G(r,\beta,t) = -\frac{\rho h}{D}\left[a_{oy} + (\dot\psi^2\sin\theta\cos\theta)r\cos\beta\cos\dot\phi t + \left(\frac{1}{2}\dot\psi^2\sin^2\theta\right)r\sin\beta\sin 2\dot\phi t\right] \quad (35)$$

Homogeneous solution

By using the method of separation of variables, it can readily be shown that the homogeneous solution of Eq. (33) for nonperforated circular plates is of the form

$$v = \sum_{m=0}^{\infty}\sum_{n=0}^{\infty}\left[\{\bar A_{mn}\sin n\beta + \bar B_{mn}\cos n\beta\}J_n\left(\alpha_{mn}\frac{r}{a}\right) + \{\bar C_{mn}\sin n\beta + \bar D_{mn}\cos n\beta\}I_n\left(\gamma_{mn}\frac{r}{a}\right)\right]F_{mn}(t) \quad (36)$$

where $\bar A_{mn}$, $\bar B_{mn}$, $\bar C_{mn}$, and $\bar D_{mn}$ are constants, J_n and I_n are Bessel functions and modified Bessel functions of order n of the first kind, respectively, and $F_{mn}(t)$ is a function of time given by the solution of the Mathieu equation

$$\ddot F_{mn}(t) + [\lambda_{mn} + B\cos 2\dot\phi t]F_{mn}(t) = 0 \quad (37)$$

where

$$\lambda_{mn} = \bar\Omega_{mn}^2 - B \quad (38)$$

$$B = (\dot\psi^2\sin^2\theta)/2 \quad (39)$$

$$\bar\Omega_{mn}^2 = \frac{D}{\rho h}\frac{\alpha_{mn}^4}{a} + \frac{T}{\rho h}\frac{\alpha_{mn}^2}{a^2} + \frac{k}{\rho h} - (\dot\phi + \dot\psi\cos\theta)^2 \quad (40)$$

In addition, the roots α_{mn} and γ_{mn} in Eq. (36) are related by Eq. (8).

The boundary conditions discussed for plates mounted perpendicular to the spin axis are equally applicable to this case. Thus, introducing Eqs. (9–17) into Eq. (36) in order to insure that the geometrical boundary conditions are satisfied, we may summarize the solution as follows:

$$v = \sum_{m=0}^{\infty}\sum_{n=0}^{\infty}\left[(\bar A_{mn}\sin n\beta + \bar B_{mn}\cos n\beta)\left\{J_n\left(\alpha_{mn}\frac{r}{a}\right) - \frac{J_n(\alpha_{mn})}{I_n(\gamma_{mn})}I_{n+1}\left(\gamma_{mn}\frac{r}{a}\right)\right\}\right]F_{mn}(t) \quad (41)$$

where $F_{mn}(t)$ is obtained from the solution of the Mathieu Eq. (37) and the roots α_{mn} and γ_{mn} are obtained as previously by simultaneously solving Eqs. (19).

Nonhomogeneous solution

Using the eigenfunctions of the homogeneous solution, the solution for forced motion is assumed in the following form:

$$v = \sum_{m=0}^{\infty}\sum_{n=0}^{\infty}[\bar A_{mn}(t)\sin n\beta + \bar B_{mn}(t)\cos n\beta]\left\{J_n\left(\alpha_{mn}\frac{r}{a}\right) - \frac{J_n(\alpha_{mn})}{I_n(\gamma_{mn})}I_n\left(\gamma_{mn}\frac{r}{a}\right)\right\} \quad (42)$$

The roots α_{mn} and γ_{mn} are given by Eqs. (19) for either simply supported or clamped edges, which insures that the geometrical boundary conditions are satisfied.

Substituting Eq. (42) into Eq. (33) and applying the same Fourier techniques as discussed in the previous section for plates mounted perpendicular to the spin axis, one obtains by virtue of the orthogonality properties discussed in the Appendix,

$$\ddot{\bar A}_{mn} + [\lambda_{mn} + B\cos 2\dot\phi t]\bar A_{mn} = \frac{D}{\rho h Q_{mn}}\int_0^{2\pi}\int_0^a \bar G(r,\beta,t)\left\{J_n\left(\alpha_{mn}\frac{r}{a}\right) - \frac{J_n(\alpha_{mn})}{I_n(\gamma_{mn})}I_n\left(\gamma_{mn}\frac{r}{a}\right)\right\}(\sin n\beta)r\,dr\,d\beta \quad (43)$$

and

$$\ddot{\bar B}_{mn} + [\lambda_{mn} + B\cos 2\dot\phi t]\bar B_{mn} = \frac{D}{\rho h Q_{mn}}\int_0^{2\pi}\int_0^a \bar G(r,\beta,t)\left\{J_n\left(\alpha_{mn}\frac{r}{a}\right) - \frac{J_n(\alpha_{mn})}{I_n(\gamma_{mn})}I_n\left(\gamma_{mn}\frac{r}{a}\right)\right\}(\cos n\beta)r\,dr\,d\beta \quad (44)$$

where λ_{mn} and B are given by Eqs. (38–40) and Q_{mn} is given by Eqs. (25) and (26) for clamped and simply supported outer edges, respectively.

Integrating the right-hand sides of Eqs. (43) and (44) yields

$$\begin{aligned}\ddot{\bar A}_{mn} + [\lambda_{mn} + B\cos 2\dot\phi t]\bar A_{mn} &= \bar A(m,n,t)\\ \ddot{\bar B}_{mn} + [\lambda_{mn} + B\cos 2\dot\phi t]\bar B_{mn} &= \bar B(m,n,t)\end{aligned} \quad (45)$$

where

$$\bar A(m,n,t) = \begin{cases} 0; & \text{for } n \neq 1 \\ -\dfrac{\pi a^3}{2Q_{m1}}\dot\psi^2\sin^2\theta\left\{\dfrac{J_2(\alpha_{m1})}{\alpha_{m1}} - \dfrac{J_1(\alpha_{m1})}{I_1(\gamma_{m1})}\dfrac{I_2(\gamma_{m1})}{\gamma_{m1}}\right\}\sin 2\dot\phi t; & \text{for } n = 1\end{cases} \quad (46)$$

$$\bar{B}(m,n,t) = \left\{ \begin{array}{l} 0; \text{ for } n \neq 1 \\ -\dfrac{\pi a^3}{Q_{m1}} \dot{\psi}^2 \sin\theta \cos\theta \left\{ \dfrac{J_2(\alpha_{m1})}{\alpha_{m1}} - \dfrac{J_1(\alpha_{m1})}{I_1(\gamma_{m1})} \dfrac{I_2(\gamma_{m1})}{\gamma_{m1}} \right\} \cos\dot{\phi}t; \text{ for } n = 1 \\ -\dfrac{2\pi a^2}{Q_{m0}} \left\{ \dfrac{J_1(\alpha_{mo})}{\alpha_{mo}} - \dfrac{J_0(\alpha_{mo})}{I_0(\gamma_{mo})} \dfrac{I_1(\gamma_{mo})}{\gamma_{mo}} \right\} a_{oy}; \text{ for } n = 0 \end{array} \right\} \quad (47)$$

Thus, as observed for plates mounted perpendicular to the spin axis only the modes corresponding to $n = 1$ are excited by the gyroscopically induced harmonic loads. However, for this case resonance may be excited at either the spin frequency $\dot{\phi}$ or at $2\dot{\phi}$. In addition, any acceleration a_{oy} of the reference origin 0 perpendicular to the plane of the plate produces an axially symmetric dynamic response.

Inspection of Eqs. (45) shows that the coefficients $\bar{A}_{mn}$ and $\bar{B}_{mn}$ must be determined by solving a Mathieu equation for each mode. Equation (45) can be written in terms of the nondimensional time variable $\tau = 2\dot{\phi}t$ as

$$\left. \begin{array}{l} \dfrac{d^2\bar{A}_{mn}}{d\tau^2} + [\delta_{mn} + \epsilon \cos\tau]\bar{A}_{mn} = \dfrac{\bar{A}(m,n,\tau)}{4\dot{\phi}^2} \\ \dfrac{d^2\bar{B}_{mn}}{d\tau^2} + [\delta_{mn} + \epsilon \cos\tau]\bar{B}_{mn} = \dfrac{\bar{B}(m,n,\tau)}{4\dot{\phi}^2} \end{array} \right\} \quad (48)$$

where

$$\delta_{mn} = \lambda_{mn}/4\dot{\phi}^2 = \bar{\Omega}_{mn}^2/4\dot{\phi}^2 - \epsilon \quad (49)$$

$$\epsilon = B/4\dot{\phi}^2 = \dot{\psi}^2 \sin^2\theta/8\dot{\phi}^2 \quad (50)$$

and $\bar{A}(m,n,\tau)$ and $\bar{B}(m,n,\tau)$ result from substituting $\tau = 2\dot{\phi}t$ into Eqs. (45).

The solution of Eqs. (48) and its stability characteristics are discussed in detail in the literature[8,9] and therefore will not be presented in depth herein. Moreover, the behavior of circular plates for this case is generally the same as that previously discussed in detail for rectangular plates.[4] However, it is interesting to note from Eqs. (49) and (50) that the stability characteristics for each mode as governed by δ_{mn} and ϵ are influenced by both precession and spin. Thus, either stable or unstable modes may readily occur.

In applications for which $\dot{\psi}^2 \sin^2\theta$ is negligible compared to $\bar{\Omega}_{mn}^2$, λ_{mn} in Eqs. (45) reduces to simply $\bar{\Omega}_{mn}^2$ given by Eq. (40) and Eqs. (45) reduce to differential equations with constant coefficients given by

$$\left. \begin{array}{l} \ddot{\bar{A}}_{mn} + \bar{\Omega}_{mn}^2\bar{A}_{mn} = \bar{A}_{mn}(m,n,t) \\ \ddot{\bar{B}}_{mn} + \bar{\Omega}_{mn}^2\bar{B}_{mn} = \bar{B}_{mn}(m,n,t) \end{array} \right\} \quad (51)$$

The particular solution of Eqs. (51) for $a_{oy} = 0$ yields the amplitude coefficients in the form

$$\left. \begin{array}{l} \bar{A}_{mn} = \bar{A}(m,n,t)/(\bar{\Omega}_{mn}^2 - \dot{\phi}^2) \\ \bar{B}_{mn} = \bar{B}(m,n,t)/(\bar{\Omega}_{mn}^2 - \dot{\phi}^2) \end{array} \right\} \quad (52)$$

where $\bar{A}(m,n,t)$ and $\bar{B}(m,n,t)$ are given by Eqs. (46) and (47). Thus, Eqs. (52) along with the well-known homogeneous solution of Eq. (51) together with Eq. (42) complete the solution for this case.

In addition, from the equation for the circular frequency $\bar{\Omega}_{mn}^2$ given by Eq. (40) it is readily seen that the natural frequency is reduced by both the effects of spin $\dot{\phi}$ and precession $\dot{\psi}$. For a plate with $T = k = 0$, this reduction in frequency is dependent on the ratio of $(\dot{\phi} + \dot{\psi}\cos\theta)$ to the flexural rigidity parameter $(D/\rho h)^{1/2}(\alpha_{mn}/a)^2$. Therefore, as previously discussed for plates mounted perpendicular to the spin axis, this effect can become significant for appropriate combinations of material properties and plate geometry even for relatively small values of spin and precession. Furthermore, by taking $D = k = 0$, Eq. (46) reduces to the equation for the circular frequency of an elastic membrane given by

$$\bar{\Omega}_{mn}^2 = (T/\rho h)(\alpha_{mn}/a)^2 - (\dot{\phi} + \dot{\psi}\cos\theta)^2 \quad (53)$$

Thus, it is easily seen that the natural frequency of a membrane can be significantly reduced by spin and precession, especially for applications for which the membrane tensions are relatively low.

III. Closure

The analysis presented herein shows that only the modes of vibration associated with the first-order Bessel function J_1 are excited by the gyroscopically induced cyclic inertia loads for circular plates mounted either perpendicular or parallel to the spin axis. The amplitude of response for plates mounted perpendicular to the spin axis is governed by ordinary differential equations with constant coefficients, whereas for members mounted parallel to the spin axis the amplitude coefficients are governed by a Mathieu equation for each mode.

The natural frequency for all cases studied is reduced by the combined effects of spin and precession and this reduction may become significant for plates with appropiate geometrical and material parameters, even for low rates of spin and precession. Furthermore, this effect becomes very important for membranes, especially when the membrane tension is low. The designer is furnished with appropriate equations from which he can determine the necessary tension that must be applied to circular plates and membranes in order to satisfy design specifications on natural frequency, taking spin and precession into account.

Appendix: Orthogonality

Referring to the table of formulas given by McLachlan,[9] the integral

$$\int_0^a \left\{ J_n\left(\alpha_{mn}\frac{r}{a}\right) - \frac{J_n(\alpha_{mn})}{I_n(\gamma_{mn})} I_n\left(\gamma_{mn}\frac{r}{a}\right) \right\} \times \left\{ J_n\left(\alpha_{sn}\frac{r}{a}\right) - \frac{J_n(\alpha_{sn})}{I_n(\gamma_{sn})} I_n\left(\gamma_{sn}\frac{r}{a}\right) \right\} rdr =$$

$$\frac{a^2}{\alpha_{mn}^2 - \alpha_{sn}^2} \{\alpha_{mn}J_{n+1}(\alpha_{mn})J_n(\alpha_{sn}) - \alpha_{sn}J_n(\alpha_{mn})J_{n+1}(\alpha_{sn})\} - \frac{J_n(\alpha_{mn})}{I_n(\gamma_{mn})} \frac{a^2}{\gamma_{mn}^2 + \alpha_{sn}^2} \{\gamma_{mn}I_{n+1}(\gamma_{mn})J_n(\alpha_{sn}) + \alpha_{sn}I_n(\gamma_{mn})J_{n+1}(\alpha_{sn})\} - \frac{J_n(\alpha_{sn})}{I_n(\gamma_{sn})} \frac{a^2}{\alpha_{mn}^2 + \gamma_{sn}^2} \times \{\alpha_{mn}J_{n+1}(\alpha_{mn})I_n(\gamma_{sn}) + \gamma_{sn}J_n(\alpha_{mn})I_{n+1}(\gamma_{sn})\} + \frac{J_n(\alpha_{mn})}{I_n(\gamma_{mn})} \frac{J_n(\alpha_{sn})}{I_n(\gamma_{sn})} \frac{a^2}{\gamma_{mn}^2 - \gamma_{sn}^2} \{\gamma_{mn}I_{n+1}(\gamma_{mn})I_n(\gamma_{sn}) - \gamma_{sn}I_n(\gamma_{mn})I_{n+1}(\gamma_{sn})\} \quad (A1)$$

for $s \neq m$. The sets of roots γ_{mn}, α_{mn}, and γ_{sn}, α_{sn} must each satisfy Eq. (15) and as a result they are related to each other by the condition that

$$\gamma_{mn}^2 - \gamma_{sn}^2 = \alpha_{mn}^2 - \alpha_{sn}^2 \quad (A2)$$

In addition, the boundary conditions at the outer edge require that each set of roots satisfy the respective equation:

$$\alpha_{mn}\frac{J_{n+1}(\alpha_{mn})}{J_n(\alpha_{mn})} + \gamma_{mn}\frac{I_{n+1}(\gamma_{mn})}{I_n(\gamma_{mn})} = \left\{\frac{\alpha_{mn}^2 + \gamma_{mn}^2}{1 - \nu}\right\}\delta \quad (A3)$$

or

$$\alpha_{sn}\frac{J_{n+1}(\alpha_{sn})}{J_n(\alpha_{sn})} + \gamma_{sn}\frac{I_{n+1}(\gamma_{sn})}{I_n(\gamma_{sn})} = \left\{\frac{\alpha_{sn}^2 + \gamma_{sn}^2}{1 - \nu}\right\}\delta \quad (A4)$$

where $\delta = 0$ for clamped edges and $\delta = 1$ for simply supported edges. Substituting Eqs. (A2, A3, and A4) into Eq. (A1), it is readily verified that for $s \neq m$

$$\int_0^a \left\{ J_n\left(\alpha_{mn}\frac{r}{a}\right) - \frac{J_n(\alpha_{mn})}{I_n(\gamma_{mn})} I_n\left(\gamma_{mn}\frac{r}{a}\right)\right\}\left\{ J_n\left(\alpha_{sn}\frac{r}{a}\right) - \frac{J_n(\alpha_{sn})}{I_n(\gamma_{sn})} I_n\left(\gamma_{sn}\frac{r}{a}\right)\right\} rdr = 0 \quad \text{(A5)}$$

for both clamped and simply supported outer edges at $r = a$.

References

[1] Hirschberg, M. H. and Mendleson, A., "Analysis of Stresses and Deflections in a Disk Subjected to Gyroscopic Forces," TN-4218, 1958, NACA.

[2] Meirovitch, L., "Bending Vibrations of a Disk Subjected to Gyroscopic Forces," *Journal of the Astronautical Sciences*, Vol. 8, 1961, pp. 88–93.

[3] Johnson, M. W., "On the Dynamics of Shallow Elastic Members," *Proceedings of the Symposium on the Theory of Thin Elastic Shells (Delft)*, North-Holland, Amsterdam, 1960, pp. 281–300.

[4] Schlack, A. L. and Kessel, P. G., "Gyroscopically Induced Vibrations of Plates and Membranes," *AIAA Journal*, Vol. 6, No. 12, Dec. 1968, pp. 2360–2363.

[5] Timoshenko, S. and Woinowsky-Kreiger, S., *Theory of Plates and Shells*, McGraw-Hill, New York, 1959.

[6] Wah, T., "Vibration of Circular Plates," *Journal of the Acoustical Society of America*, Vol. 34, No. 3, 1962, pp. 275–281.

[7] Weiner, R. S., "Forced Axisymmetric Motions of Circular Elastic Plates," *Journal of Applied Mechanics*, Vol. 4, 1965, pp. 893–898.

[8] Stoker, J. J., *Nonlinear Vibrations*, Interscience, New York, 1950, Chap. VI.

[9] McLachlan, N. W., *Theory and Applications of Mathieu Functions*, Dover, New York, 1964.

OCTOBER 1969 AIAA JOURNAL VOL. 7, NO. 10

A Penetration Criterion for Double-Walled Structures Subject to Meteoroid Impact

J. P. D. WILKINSON*
General Electric Company, Schenectady, N.Y.

A penetration criterion is developed for double-walled structures subject to hypervelocity impact. During the impact, both the incoming particle and a portion of the front sheet are fragmented, and the resulting spray loads the rear sheet impulsively. The rear sheet is said to have failed when the strain it experiences exceeds the strain-to-fracture of the material. In this study the rear sheet response is followed into the elasto-plastic regime by means of an existing computer code. Based on the new criterion, it is shown how a rational choice of material properties may be made for the front and rear sheets of the structure. Finally, the penetration criterion is applied to the problem of calculating the optimum protection requirements for given spacecraft applications during interplanetary flight. Here, a Monte Carlo method is used to account for the observed distribution of meteoroid properties.

Nomenclature

A = exposed area
a,b = flux constants
c_1,c_2 = speed of sound in front and rear sheets
d = particle diameter
E = Young's modulus
m = particle mass
m_1 = mass per unit area of front sheet
m_2 = mass per unit area of rear sheet
m_* = mass of plug removed from front sheet
N = cumulative number of meteoroids
P_n = probability of n events or fewer
r = radial distance from impact point
S = spacing between front and rear sheets
T = time of exposure
t_1,t_2 = thickness of front and rear sheets
V = particle velocity
$\bar{V}_A$ = average axial spray velocity
$\bar{V}_R$ = average radial spray velocity
Δ = standard deviation of spray mass distribution
ϵ = strain, or ductility, or elongation
$\epsilon_{\max}$ = maximum strain experienced by rear sheet
$\bar{\theta}$ = average cone angle of spray
ν = Poisson's ratio
ρ = particle density
ρ_1,ρ_2 = densities of front and rear sheets
σ = initial biaxial stress state due to pressurization
σ_u = ultimate stress
σ_y = yield stress
σ_{yt} = yield stress at 0.2% offset

Presented as Paper 68-1058 at the AIAA 5th Annual Meeting and Technical Display, Philadelphia, Pa., October 21–24, 1968; submitted September 27, 1968; revision received April 14, 1969. The author wishes to thank J. A. Mirabal and S. R. Woodall for their constructive suggestions and criticisms during the course of this investigation.

* Mechanical Engineer, Research and Development Center. Member AIAA.

Introduction

DURING a long interplanetary mission, there is, according to the best data available, a distinct possibility that a spacecraft will encounter meteoroids of such a size that considerable damage could be caused if adequate protection is not given to the spacecraft, its electronic components, and its fuel tanks. One way of doing this is to erect a thin shield a certain distance from the main structure. The shield then serves to fragment and perhaps vaporize an incoming hypervelocity particle, and the resulting debris spreads out in the form of a cone. The damage to the rear wall is thus considerably less than if the wall were unshielded.

The calculation of the penetration mechanics of a hypervelocity particle into such a structure is extremely complex. Several numerical methods based essentially on the hydro-